Molecular Switches

International Edition: DOI: 10.1002/anie.201604290
German Edition: DOI: 10.1002/ange.201604290

Photoswitchable NIR-Emitting Gold Nanoparticles

*Sara Bonacchi, Andrea Cantelli, Giulia Battistelli, Gloria Guidetti, Matteo Calvaresi, Jeannette Manzi, Luca Gabrielli, Federico Ramadori, Alessandro Gambarin, Fabrizio Mancin, and Marco Montalti**

Abstract: *Photo-switching of the NIR emission of gold nanoparticles (GNP) upon photo-isomerization of azobenzene ligands, bound to the surface, is demonstrated. Photophysical results confirm the occurrence of an excitation energy transfer process from the ligands to the GNP that produces sensitized NIR emission. Because of this process, the excitation efficiency of the gold core, upon excitation of the ligands, is much higher for the trans form than for the cis one, and t→c photo-isomerization causes a relevant decrease of the GNP NIR emission. As a consequence, photo-isomerization can be monitored by ratiometric detection of the NIR emission upon dual excitation. The photo-isomerization process was followed in real-time through the simultaneous detection of absorbance and luminescence changes using a dedicated setup. Surprisingly, the photo-isomerization rate of the ligands, bound to the GNP surface, was the same as measured for the chromophores in solution. This outcome demonstrated that excitation energy transfer to gold assists photo-isomerization, rather than competing with it. These results pave the road to the development of new, NIR-emitting, stimuli-responsive nanomaterials for theranostics.*

Stimuli-responsive molecular, supramolecular, and nanostructured systems are drawing increasing attention, in view of their application in fields of high economic and social impacts as materials and life sciences.[1] Light[2] offers several advantages compared to other forms of stimulation (such as electrical,[3] thermal,[4] pH,[5] pressure,[6] redox).[7] Light beams, in fact, are minimally invasive, remotely addressable, and focusable with high spatio-temporal resolution. Moreover, wavelength selection can permit multiplexed detection.[8] Additionally, multi-functionality can be achieved by combining photo-activatable and photoluminescent components. This approach is typically exploited in nanomedicine to design theranostic nanoparticles (NPs) suitable both as luminescent contrast agents for imaging[9] as well as inducible vectors for the delivery of therapeutic cargos.[10] For this kind of application, the development of NPs with tailored emission in the near-infrared region (NIR) is essential because the transparency of biological tissues is optimal in this spectral window.[11]

The photo-isomerization (PI) of azobenzene[12] (AB) has been widely exploited to control and tune the properties of materials[13] in order to perform different functions, including drug controlled release.[8b] A large variety of hybrid nanosystems that join the unique optical and electronic properties of gold nanoparticles (GNP) to the photochemical activity of AB have been developed.[1c,13d,14] Nevertheless, examples of architectures that combine the well documented NIR emission of small ($d < 2$ nm) GNP[15] to the photo-responsivity of AB are very rare[16] and, in particular, the possibility of switching the NIR luminescence of GNP upon PI of surface-bound AB units has never been demonstrated before.

Herein, we report the photophysical and photochemical properties of a newly synthesized class of luminescent GNP, stabilized with the AB-containing thiolate **A** (Scheme 1). Our results demonstrate that, upon excitation of the ligands, sensitized NIR emission of the GNP is observed thanks to an efficient energy transfer (ET) process.[17] As a consequence, the NIR luminescence of GNP can be switched ON/OFF by alternating from UV to blue irradiation. Furthermore, the isomerization state of the NPs can be monitored by ratiometric detection of the NIR luminescence (Scheme 1).

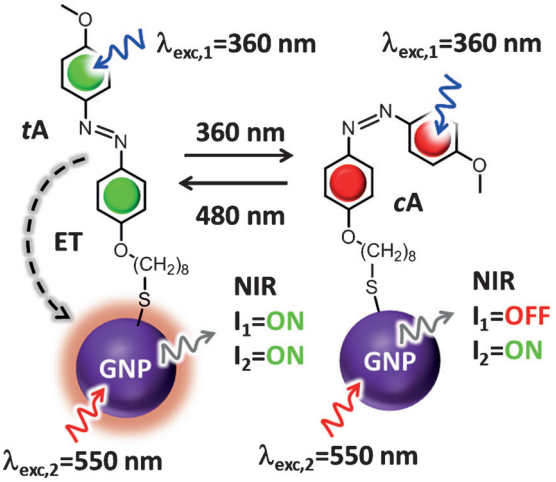

Scheme 1. Chemical formula of the *trans* azobenzene ***t*A** and of its *cis* isomer ***c*A** bound to GNP. When the ligands are in the *trans* form (left, ***t*A**-GNP, ON state) ET from ***t*A** to the GNP produces NIR-sensitized emission upon ligand excitation. Such contributions, owing to sensitization, are lost upon PI in ***c*A** covered NPs (right, ***c*A**-GNP, OFF state).

[*] Dr. S. Bonacchi, Dr. A. Cantelli, Dr. G. Battistelli, G. Guidetti, Dr. M. Calvaresi, J. Manzi, Prof. M. Montalti
Department of Chemistry "G. Ciamician"
University of Bologna
Via Selmi 2, 40126 Bologna (Italy)
E-mail: marco.montalti2@unibo.it
L. Gabrielli, Dr. F. Ramadori, Dr. A. Gambarin, Prof. F. Mancin
Department of Chemical Sciences, Università degli Studi di Padova (Italy)
Supporting information and the ORCID identification number(s) for the author(s) of this article can be found under http://dx.doi.org/10.1002/anie.201604290.

The thermodynamically stable, **A** *trans* isomer, ***t*A** showed, in $CHCl_3$ solution, the typical absorption band of AB dyes with a maximum at 360 nm and $\varepsilon = 2.7 \times 10^4\,M^{-1}\,cm^{-1}$.[12a] A gradual decrease of the intensity of this band was observed, as reported for similar molecules, upon irradiation at 360 nm, because of $t \rightarrow c$ PI. At the photostationary state (PSS), the absorbance at 360 nm was decreased to about 5% of the initial one. This observation allowed us to conclude that: i) almost complete $t \rightarrow c$ conversion occurred at the PSS, and ii) the molar absorption coefficient of ***c*A** at 360 nm was negligible with respect to the one of ***t*A**.

Going more into detail, the absorption spectra recorded at different irradiation times (see the Supporting Information) showed two isosbestic points at 320 nm and 429 nm. This behavior demonstrated that only the two species ***t*A** and ***c*A** were present in the solution, while no side photo-products were formed upon irradiation. Moreover, the absorption spectrum at the PSS strongly resembles ***c*A**. This spectrum showed two peaks at 314 nm and 448 nm ($\varepsilon = 1.0 \times 10^4\,M^{-1}\,cm^{-1}$ and $\varepsilon = 3.0 \times 10^3\,M^{-1}\,cm^{-1}$ respectively). The measured PI quantum yield was $\Phi_{t\text{-}c} = 0.15$, as reported for analogous AB derivatives.[12a] No fluorescence was observed either for ***t*A** ($\lambda_{exc} = 360$ nm) or for ***c*A** ($\lambda_{exc} = 480$ nm).

As far as the NPs are concerned, the absorption spectrum of the ***t*A**-coated nanoclusters ***t*A**-GNP (average diameter of the gold core 1.7 nm, estimated formula Au_{144}***t*A**$_{60}$) presented, in $CHCl_3$, both the band at 360 nm of the ***t*A** chromophore and the weak surface plasmon resonance band of the gold core,[18] with the latter one dominant in the region above 550 nm (Figure 1). More precisely, the absorption spectrum of ***t*A**-GNP matches the one calculated for Au_{144}***t*A**$_{60}$ as the linear combination of the spectra of ***t*A** and of a reference sample of $CH_3(CH_2)_{11}SH$-stabilized GNP (Figure 1). This spectral matching, and thus the lack of spectral perturbation, showed that electronic interactions between adjacent ***t*A** units, as well as between ***t*A** and the gold core, were weak in the ground state.

To investigate the influence of the binding to the GNP on the PI $t \rightarrow c$ process, ***t*A**-GNP were irradiated at 360 nm in the same conditions used for the reference compound ***t*A**. As shown in Figure 1, the peaks at 314 nm and 448 nm, typical of ***c*A**, were observed at the PSS. Moreover, the same two isosbestic points at 319 nm and 430 nm, observed during the PI of the free ligand ***t*A,** were maintained during the irradiation of ***t*A**-GNP. In particular, at the PSS, the absorption spectrum of the NPs (***c*A**-GNP) perfectly matched the one expected in the case of $> 95\%$ $t \rightarrow c$ conversion. The large extent of photoswitching was the result of specific engineering of the ligand, according to studies previously reported for analogous 4,4′-dialcoxiazobenzene derivatives.[19] Interestingly, the PI quantum yield measured for ***t*A**-GNP was $\Phi_{t\text{-}c} = 0.15$, a value that matched the one observed for the reference compound ***t*A**.

As far as luminescence is concerned, a broad emission band in the NIR region, with maximum at about 930 nm, was observed upon excitation of either ***t*A**-GNP or ***c*A**-GNP in $CHCl_3$. The emission spectral profile was, for both of the samples, independent of the excitation wavelength, in the 300–600 nm range, and consistent with data reported for similar gold NPs.[15d] To investigate the effect of ligand PI on the NIR luminescence, we compared the emission spectra of the same sample of NPs recorded first at the thermodynamically stable state (***t*A**-GNP) and then at the PSS (***c*A**-GNP). The emission spectra acquired upon direct excitation of the gold core ($\lambda_{exc,2} = 550$ nm, where absorption by the ligands is negligible) were identical within the experimental error (see the Supporting Information). On the contrary, upon excitation at 360 nm, a decrease of about 60% of the intensity of the emission band was observed going from ***t*A**-GNP to ***c*A**-GNP as an effect of the $t \rightarrow c$ PI (Figure 2). These observations allowed us to conclude that: i) the emission quantum yield of the gold NP did not change because of the PI, and ii) part of the excitation energy adsorbed by ***t*A** was transferred to the gold leading to sensitized emission. Sensitization was con-

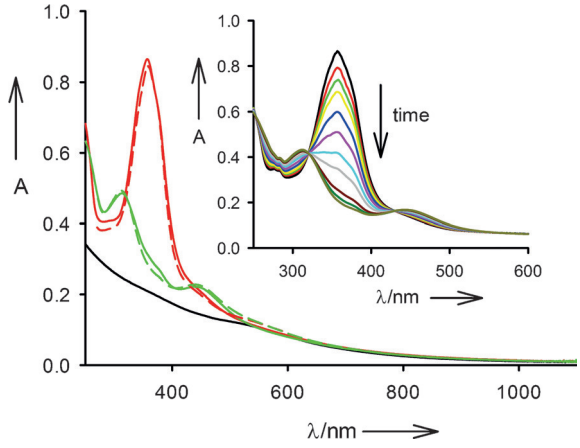

Figure 1. Continuous lines: absorption spectra of the thermodynamically stable ***t*A**-GNP in $CHCl_3$ (red) of the photo-isomerized NPs ***c*A**-GNP (green) and of reference $CH_3(CH_2)_{11}SH$ stabilized GNP (black) Dashed lines: linear combinations of the absorption spectrum of the reference GNP with those of the ligands ***t*A** (red) and ***c*A** (green). Inset: Absorption spectra of a $CHCl_3$ solution of ***t*A**-GNP during irradiation at 360 nm.

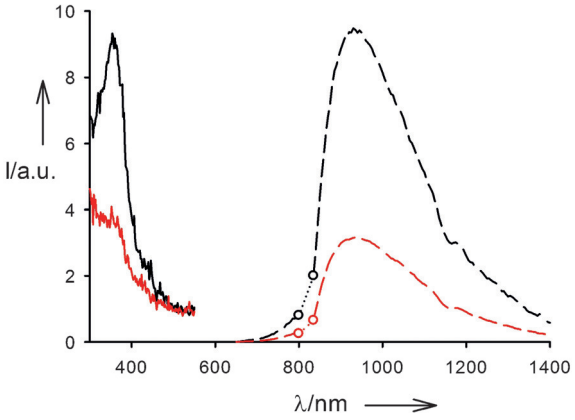

Figure 2. Continuous lines: excitation spectra of the thermodynamically stable ***t*A**-GNP in $CHCl_3$ (black) and of the photo-isomerized NPs ***c*A**-GNP (red). Dashed lines: luminescence spectra ($\lambda_{exc} = 360$ nm) of the thermodynamically stable ***t*A**-GNP in $CHCl_3$ (black) and of the photo-isomerized NPs ***c*A**-GNP (red).

firmed by the excitation spectrum of the NIR emission (Figure 2), where the band corresponding to the absorption of ***t*A** was clearly detectable in the ***t*A**-GNP. In contrast, the typical absorption band at 450 nm of the *cis* form ***c*A** was not observed in the excitation spectrum of the photo-isomerized NPs ***c*A**-GNP (Figure 2), indicating a poor contribution due to sensitized emission.

Although the mechanism of excitation ET toward GNP is still debated,[20] the poor sensitization observed in the case of ***c*A**-GNP is consistent with the following observations: i) ***c*A** electronic transition centered at 450 nm is forbidden (n-π),[12a] and thus its contribution to the overall excitation efficiency of the ***c*A**-GNP is minor. ii) MD simulation (see the Supporting Information) demonstrated that a major fraction of AB molecules are closer to the metal core in ***t*A**-GNP than in ***c*A**-GNP. iii) Much shorter excited state lifetimes have been reported for the *cis* than for the *trans* form of AB.[12a] As a consequence, independent of the model,[20] ET efficiency is expected to be much lower for the same ET constant rate in the case of ***c*A** with respect to ***t*A** (Supporting Information).

A dedicated experimental setup, suitable for simultaneously detecting light transmitted and emitted by the NPs samples during irradiation (Figure 3, inset), was developed in order to demonstrate, definitively, the correlation between the PI process and the NIR luminescence changes.

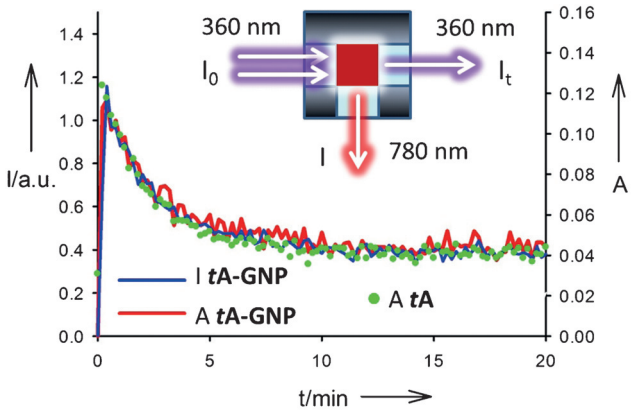

Figure 3. Changes in the photophysical properties of ***t*A**-GNP during irradiation at 360 nm in $CHCl_3$. The setup used for the measurements is shown in the inset. The fraction of irradiation light (I_0) transmitted by the sample I_t is used to measure the absorbance in real time ($A = -\log I_0/I_t$, red line). Luminescence at 780 nm is also measured in real-time (I, blue line). The absorbance changes of a $CHCl_3$ solution of ***t*A** during irradiation at 360 nm were also measured (green dots).

Absorbance and emission data recorded for ***t*A**-GNP during irradiation were compared with the absorbance values measured for ***t*A** in the same conditions (Figure 3). The good overlap between the normalized absorbance and luminescence plots for ***t*A**-GNP confirmed the correlation between the PI process and the decrease of the luminescence intensity of the GNP.

Both absorbance and luminescence plots could be fitted with an exponential decay with a rate constant $k = 0.43 \pm 0.03\ min^{-1}$. Interestingly, absorbance changes measured for the reference compound ***t*A** showed the same kinetics as ***t*A**-GNP (Figure 3), with a decay constant $k = 0.42 \pm 0.03\ min^{-1}$. These results confirmed that the rate of the $t \rightarrow c$ PI process for ***t*A**, bound to the GNP surface, was identical to one measured for the molecule free in solution.

Upon irradiation of ***c*A**-GNP at 480 nm, $c \rightarrow t$ PI occurred and about 70% of ***c*A** was converted into ***t*A** at the PSS. To further investigate the reversibility of the system, we performed a series of PI cycles by detecting the GNP emission intensity upon excitation either at $\lambda_{exc,1} = 360$ nm or $\lambda_{exc,2} = 550$ nm (I_1 and I_2 respectively). Thus, we calculated the concentration-independent ratiometric signal I_1/I_2, which is potentially useful for theranostic applications (Figure 4, red

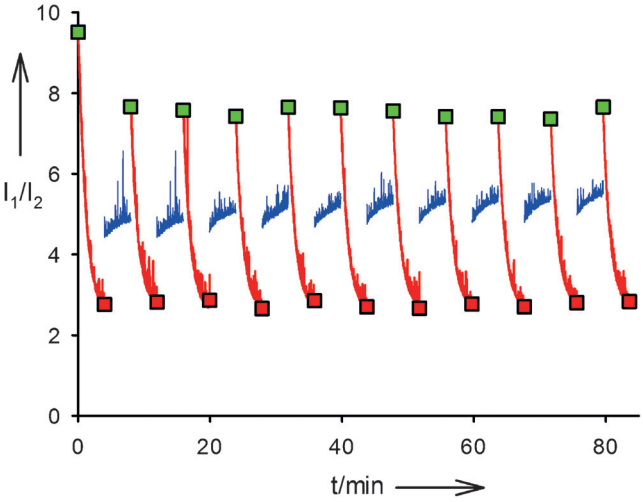

Figure 4. NIR luminescence intensity ratio upon excitation at $\lambda_{exc,1}$ ($\lambda_{exc,1} = 360$ nm for the red tracks and $\lambda_{exc,1} = 480$ nm for the blue tracks, intensity I_1 is measured at 780 nm) and $\lambda_{exc,2} = 550$ (intensity I_2 at 780 nm) of ***t*A**-GNP in $CHCl_3$. Squares show the emission intensity at the beginning (green) and at the end (red) of each irradiation cycle at 360 nm ($t \rightarrow c$ PI).

lines). Regeneration of the *trans* form was achieved by irradiation at $\lambda_{exc,1} = 480$ nm (Figure 4, blue lines). As shown in Figure 4, the NIR emission decreased upon irradiation/excitation at 360 nm. In particular, starting from ***t*A**-GNP, an intensity decrease of about 70% was observed in the first 240 s, because of the isomerization of ***t*A** and the consequent loss of the sensitized emission. During the following 240 s of irradiation/excitation at 480 nm, the NIR emission intensity increased slightly, because only poor sensitization of the gold emission occurred. After that, 360 nm excitation was restored and a strong increase of the ratiometric signal, with respect to the final value of the previous UV irradiation cycle, was observed.

To summarize, the NIR emission of the GNP can be reversibly switched from ON (Figure 4, green squares) to OFF (Figure 4, red squares) by alternating between UV and Vis irradiation. Moreover, the I_1/I_2 value at $\lambda_{exc,1} = 360$ nm and $\lambda_{exc,2} = 550$ nm can be clearly used as an isomerization state indicator.

In conclusion, we demonstrated that PI of the AB derivative ***t*A** bound to GNP occurred efficiently in our

system. The conversion of ***t*A**-GNP into ***c*A**-GNP took place almost quantitatively (> 95 %) with a quantum yield identical to the one measured for ***t*A** in solution (upon irradiation at 360 nm). Regeneration of 70 % of ***t*A**-GNP was, in turn, achieved by irradiation of ***c*A**-GNP at 480 nm. Photoluminescence measurements showed that ***t*A**-GNP emitted in the NIR region upon direct excitation of the gold core ($\lambda_{exc,2}$ = 550 nm) and that, upon excitation of the ***t*A** ligand ($\lambda_{exc,1}$ = 360 nm), an ET process from the molecular ligand to the metal core occurred, producing sensitized NIR emission. Thanks to this process, the ratio of the emission intensity, measured in the two different excitation conditions (either $\lambda_{exc,1}$ or $\lambda_{exc,2}$) could be used to detect the isomerization state of the NPs. Ratiometric detection offers several advantages with respect to single-wavelength detection, including concentration-independent responses. Surprisingly, the lack of any effect of the binding to GNP on the PI rate of ***t*A** suggested that the ET process to gold assisted the PI rather than competing with it.

Finally, although the typically modest luminescence quantum yield of GNP[15d,21] needs to be improved to make them competitive with other systems for in vivo applications,[11c,e,22] we believe that the results we reported here pave the road to the development of new NIR-emitting stimuli-responsive nanomaterials for combined diagnostics and therapeutics.

Acknowledgements

The research leading to these results has received funding from the European Union Seventh Framework Programme under grant agreement no. 604391 Graphene Flagship. We gratefully acknowledge financial support from ERC ("MOSAIC" Starting Grant 259014).

Keywords: gold · luminescence · nanoparticles · near infrared · stimuli-responsive compounds

How to cite: *Angew. Chem. Int. Ed.* **2016**, *55*, 11064–11068
Angew. Chem. **2016**, *128*, 11230–11234

[1] a) E. Borré, J. F. Stumbé, S. Bellemin-Laponnaz, M. Mauro, *Angew. Chem. Int. Ed.* **2016**, *55*, 1313 – 1317; *Angew. Chem.* **2016**, *128*, 1335 – 1339; b) G. S. Kumar, D. C. Neckers, *Chem. Rev.* **1989**, *89*, 1915 – 1925; c) J. Zhang, J. K. Whitesell, M. A. Fox, *Chem. Mater.* **2001**, *13*, 2323 – 2331; d) A. P. Blum, J. K. Kammeyer, A. M. Rush, C. E. Callmann, M. E. Hahn, N. C. Gianneschi, *J. Am. Chem. Soc.* **2015**, *137*, 2140 – 2154; e) L. D. Zarzar, J. Aizenberg, *Acc. Chem. Res.* **2014**, *47*, 530 – 539; f) J.-M. Lehn, *Angew. Chem. Int. Ed.* **2015**, *54*, 3276 – 3289; *Angew. Chem.* **2015**, *127*, 3326 – 3340; g) M. Montalti, G. Battistelli, A. Cantelli, D. Genovese, *Chem. Commun.* **2014**, *50*, 5326 – 5329; h) H. Kumari, S. R. Kline, S. R. Kennedy, C. Garvey, C. L. Raston, J. L. Atwood, J. W. Steed, *Chem. Commun.* **2016**, *52*, 4513 – 4516; i) G. O. Lloyd, J. W. Steed, *Nat. Chem.* **2009**, *1*, 437 – 442.

[2] a) S. V. Aradhya, L. Venkataraman, *Nat. Nanotechnol.* **2013**, *8*, 399 – 410; b) Y. Wu, Y. Xie, Q. Zhang, H. Tian, W. Zhu, A. D. Q. Li, *Angew. Chem. Int. Ed.* **2014**, *53*, 2090 – 2094; *Angew. Chem.* **2014**, *126*, 2122 – 2126; c) S. J. Wezenberg, K.-Y. Chen, B. L. Feringa, *Angew. Chem. Int. Ed.* **2015**, *54*, 11457 – 11461; *Angew. Chem.* **2015**, *127*, 11619 – 11623; d) W. A. Velema, J. P. van der Berg, W. Szymanski, A. J. M. Driessen, B. L. Feringa, *ACS Chem. Biol.* **2014**, *9*, 1969 – 1974; e) W. A. Velema, J. P. van der Berg, M. J. Hansen, W. Szymanski, A. J. M. Driessen, B. L. Feringa, *Nat. Chem.* **2013**, *5*, 924 – 928.

[3] S. Taccola, F. Greco, E. Sinibaldi, A. Mondini, B. Mazzolai, V. Mattoli, *Adv. Mater.* **2015**, *27*, 1668 – 1675.

[4] C. A. Figg, A. Simula, K. A. Gebre, B. S. Tucker, D. M. Haddleton, B. S. Sumerlin, *Chem. Sci.* **2015**, *6*, 1230 – 1236.

[5] M. Kanamala, W. R. Wilson, M. Yang, B. D. Palmer, Z. Wu, *Biomaterials* **2016**, *85*, 152 – 167.

[6] Y. Wang, X. Tan, Y.-M. Zhang, S. Zhu, I. Zhang, B. Yu, K. Wang, B. Yang, M. Li, B. Zou, S. X.-A. Zhang, *J. Am. Chem. Soc.* **2015**, *137*, 931 – 939.

[7] K. Miyamae, M. Nakahata, Y. Takashima, A. Harada, *Angew. Chem. Int. Ed.* **2015**, *54*, 8984 – 8987; *Angew. Chem.* **2015**, *127*, 9112 – 9115.

[8] a) D. Bléger, S. Hecht, *Angew. Chem. Int. Ed.* **2015**, *54*, 11338 – 11349; *Angew. Chem.* **2015**, *127*, 11494 – 11506; b) W. A. Velema, W. Szymanski, B. L. Feringa, *J. Am. Chem. Soc.* **2014**, *136*, 2178 – 2191; c) M. Baroncini, S. O'Agostino, G. Bergamini, P. Ceroni, A. Comotti, P. Sozzani, I. Bassanetti, F. Grepioni, T. M. Hernandez, S. Silvi, M. Venturi, A. Credi, *Nat. Chem.* **2015**, *7*, 634 – 640; d) V. Balzani, G. Bergamini, P. Ceroni, *Angew. Chem. Int. Ed.* **2015**, *54*, 11320 – 11337; *Angew. Chem.* **2015**, *127*, 11474 – 11492.

[9] Z. Tian, A. D. Q. Li, *Acc. Chem. Res.* **2013**, *46*, 269 – 279.

[10] a) R. Lehner, X. Wang, M. Wolf, P. Hunziker, *J. Controlled Release* **2012**, *161*, 307 – 316; b) C. Stoffelen, J. Voskuhl, P. Jonkheijm, J. Huskens, *Angew. Chem. Int. Ed.* **2014**, *53*, 3400 – 3404; *Angew. Chem.* **2014**, *126*, 3468 – 3472.

[11] a) V. Shanmugam, S. Selvakumar, C. S. Yeh, *Chem. Soc. Rev.* **2014**, *43*, 6254 – 6287; b) D. M. Yang, P. A. Ma, Z. Y. Hou, Z. Y. Cheng, C. X. Li, J. Lin, *Chem. Soc. Rev.* **2015**, *44*, 1416 – 1448; c) M. Montalti, A. Cantelli, G. Battistelli, *Chem. Soc. Rev.* **2015**, *44*, 4853 – 4921; d) M. Montalti, L. Prodi, E. Rampazzo, N. Zaccheroni, *Chem. Soc. Rev.* **2014**, *43*, 4243 – 4268; e) E. Rampazzo, F. Boschi, S. Bonacchi, R. Juris, M. Montalti, N. Zaccheroni, L. Prodi, L. Calderan, B. Rossi, S. Becchi, A. Sbarbati, *Nanoscale* **2012**, *4*, 824 – 830; f) D. Genovese, S. Bonacchi, R. Juris, M. Montalti, L. Prodi, E. Rampazzo, N. Zaccheroni, *Angew. Chem. Int. Ed.* **2013**, *52*, 5965 – 5968; *Angew. Chem.* **2013**, *125*, 6081 – 6084.

[12] a) H. M. D. Bandara, S. C. Burdette, *Chem. Soc. Rev.* **2012**, *41*, 1809 – 1825; b) S. Castellanos, A. Goulet-Hanssens, F. Zhao, A. Dikhtiarenko, A. Pustovarenko, S. Hecht, J. Gascon, F. Kapteijn, D. Bleger, *Chem. Eur. J.* **2016**, *22*, 746 – 752; c) S. Fredrich, R. Goestl, M. Herder, L. Grubert, S. Hecht, *Angew. Chem. Int. Ed.* **2016**, *55*, 1208 – 1212; *Angew. Chem.* **2016**, *128*, 1226 – 1230; d) C.-L. Lee, T. Liebig, S. Hecht, D. Bleger, J. P. Rabe, *ACS Nano* **2014**, *8*, 11987 – 11993; e) J. Moreno, M. Gerecke, L. Grubert, S. A. Kovalenko, S. Hecht, *Angew. Chem. Int. Ed.* **2016**, *55*, 1544 – 1547; *Angew. Chem.* **2016**, *128*, 1569 – 1573.

[13] a) W. Feng, W. Luo, Y. Feng, *Nanoscale* **2012**, *4*, 6118 – 6134; b) F. D. Jochum, P. Theato, *Chem. Soc. Rev.* **2013**, *42*, 7468 – 7483; c) W.-P. Lin, S.-J. Liu, T. Gong, Q. Zhao, W. Huang, *Adv. Mater.* **2014**, *26*, 570 – 606; d) M. Döbbelin, A. Ciesielski, S. Haar, S. Osella, M. Bruna, A. Minoia, L. Grisanti, T. Mosciatti, F. Richard, E. A. Prasetyanto, L. De Cola, V. Palermo, R. Mazzaro, V. Morandi, R. Lazzaroni, A. C. Ferrari, D. Beljonne, P. Samori, *Nat. Commun.* **2016**, *7*, 11090.

[14] a) G. K. Joshi, K. N. Blodgett, B. B. Muhoberac, M. A. Johnson, K. A. Smith, R. Sardar, *Nano Lett.* **2014**, *14*, 532 – 540; b) G. L. Hallett-Tapley, C. D'Alfonso, N. L. Pacioni, C. D. McTiernan, M. Gonzalez-Bejar, O. Lanzalunga, E. I. Alarcon, J. C. Scaiano, *Chem. Commun.* **2013**, *49*, 10073 – 10075; c) D. T. Valley, M. Onstott, S. Malyk, A. V. Benderskii, *Langmuir* **2013**, *29*, 11623 –

11631; d) Y. Q. Yan, J. I. L. Chen, D. S. Ginger, *Nano Lett.* **2012**, *12*, 2530 – 2536; e) C. Raimondo, B. Kenens, F. Reinders, M. Mayor, H. Uji-i, P. Samori, *Nanoscale* **2015**, *7*, 13836 – 13839; f) N. Crivillers, S. Osella, C. Van Dyck, G. M. Lazzerini, D. Cornil, A. Liscio, F. Di Stasio, S. Mian, O. Fenwick, F. Reinders, M. Neuburger, E. Treossi, M. Mayor, V. Palermo, F. Cacialli, J. Cornil, P. Samori, *Adv. Mater.* **2013**, *25*, 432 – 436; g) C. Raimondo, N. Crivillers, F. Reinders, F. Sander, M. Mayor, P. Samori, *Proc. Natl. Acad. Sci. USA* **2012**, *109*, 12375 – 12380; h) C. Raimondo, F. Reinders, U. Soydaner, M. Mayor, P. Samori, *Chem. Commun.* **2010**, *46*, 1147 – 1149.

[15] a) R. Khandelia, S. Bhandari, U. N. Pan, S. S. Ghosh, A. Chattopadhyay, *Small* **2015**, *11*, 4075 – 4081; b) Z. K. Wu, R. C. Jin, *Nano Lett.* **2010**, *10*, 2568 – 2573; c) G. L. Wang, T. Huang, R. W. Murray, L. Menard, R. G. Nuzzo, *J. Am. Chem. Soc.* **2005**, *127*, 812 – 813; d) M. Montalti, N. Zaccheroni, L. Prodi, N. O'Reilly, S. L. James, *J. Am. Chem. Soc.* **2007**, *129*, 2418 – 2419; e) K. Saha, S. S. Agasti, C. Kim, X. N. Li, V. M. Rotello, *Chem. Rev.* **2012**, *112*, 2739 – 2779.

[16] Y. Negishi, U. Kamimura, M. Ide, M. Hirayama, *Nanoscale* **2012**, *4*, 4263 – 4268.

[17] E. Rampazzo, S. Bonacchi, R. Juris, M. Montalti, D. Genovese, N. Zaccheroni, L. Prodi, D. C. Rambaldi, A. Zattoni, P. Reschiglian, *J. Phys. Chem. B* **2010**, *114*, 14605 – 14613.

[18] a) N. K. Chaki, Y. Negishi, H. Tsunoyama, Y. Shichibu, T. Tsukuda, *J. Am. Chem. Soc.* **2008**, *130*, 8608 – 8610; b) H. Qian, R. Jin, *Nano Lett.* **2009**, *9*, 4083 – 4087; c) L. M. Tvedte, C. J. Ackerson, *J. Phys. Chem. A* **2014**, *118*, 8124 – 8128.

[19] a) J. Dokić, M. Gothe, J. Wirth, M. V. Peters, J. Schwarz, S. Hecht, P. Saalfrank, *J. Phys. Chem. A* **2009**, *113*, 6763 – 6773; b) C. Dri, M. V. Peters, J. Schwarz, S. Hecht, L. Grill, *Nat. Nanotechnol.* **2008**, *3*, 649 – 653.

[20] a) T. L. Jennings, M. P. Singh, G. F. Strouse, *J. Am. Chem. Soc.* **2006**, *128*, 5462 – 5467; b) A. Samanta, Y. D. Zhou, S. L. Zou, H. Yan, Y. Liu, *Nano Lett.* **2014**, *14*, 5052 – 5057.

[21] Y. Cheng, G. Lu, Y. He, H. Shen, J. Zhao, K. Xia, Q. Gong, *Nanoscale* **2016**, *8*, 2188 – 2194.

[22] a) Z. Guo, S. Park, J. Yoon, I. Shin, *Chem. Soc. Rev.* **2014**, *43*, 16 – 29; b) L. Yuan, W. Lin, K. Zheng, L. He, W. Huang, *Chem. Soc. Rev.* **2013**, *42*, 622 – 661.

Received: May 3, 2016
Revised: June 9, 2016
Published online: August 11, 2016

